No. 3/86

EVALUATION OF ADVANCED SODIUM RECEIVER LOSSES DURING OPERATION

R. CARMONA, F. ROSA, H. JACOBS, AND M. SÁNCHEZ

IEA - OPERATING AGENT

C. I. E. M. A. T.

INSTITUTO DE ENERGIAS RENOVABLES

SSPS Technical Report No. 3/86

EVALUATION OF ADVANCED SODIUM RECEIVER LOSSES DURING OPERATION

R. Carmona, F. Rosa, H. Jacobs, and M. Sánchez

CONTENTS :

1. INTRODUCTION

The basis of the experiment reported here was to provide loss measurements used to determine the receiver performances. Two sodium receivers have been tested in the SSPS Project. A cavity receiver (designed by INTERATOM and constructed by SULZER) and an external receiver (designed and manufactured by Franco-Tosi).Results from the cavity receiver have previously been reported (Ref.1). This paper presents the measurements and experiments conducted with the external receiver, a billboard type, called the Advanced Sodium Receiver (ASR).

Optical losses and subsequent degradation were assessed using absorptance measurements of the receiver coating. Two sets of measurements were made: the first after 1,000 hours of operation under normal conditions; and the second after testing the receiver above design conditions, after the so-called High Flux Experiment (HFE).

A variety of techniques have been used or suggested to measure convective losses of the central receiver (Ref.2). Most of these techniques are not sufficiently accurate to produce meaningful results. Because of uncertainties in the incoming flux measurements, the flux-off technique seems best suited for estimating thermal losses in a central receiver. The test consists in operation of the receiver, opening the doors and circulating the sodium in normal and reverse flow without providing any incident power from the heliostat field.

Radiative losses can be accurately calculated for a billboard receiver. The method used is based on theoretical calculations and some results have been compared with infrared thermography measurements. Conductive losses are small and can also be estimated by flux-off experiment with the doors closed.

2. OPTICAL LOSSES

To determine the optical losses in the ASR, absorptance measurements have been carried out using a Solar Spectrum Reflectometer, developed by Devices and Services, Co., Dallas, Texas. This instrument measures the hemispherical directional reflectance averaged over a simulated Air Mass 2 spectrum.

The first measurement campaign was performed in January 1985, after 1,000 hours of operation. The second campaign took place in January 1986, after completion of the HFE.

A method has been developed on site for estimating the absorptance distribution. It aims to:

- estimate the distribution of the absorptance over a surface from discrete measurement points, and
- ascertain the zones of homogenous absorptance, within an accurate and confident range.

A computer code was developed for this purpose, MLRAD. This program defines this surface by a linear method based on planes defined by three measurements. To obtain the absorptance distribution of zones at different confidence levels the standard statistical method, 'variance analysis', was applied.

A set of 165 measurement points were selected on the whole receiver to determine the absorptance distribution. Due to the more critical position of the fifth panel (central panel), a second set of 189 points were taken from this panel. So that the results of the measurements could be compared with the values obtained from a new panel, 62 samples were taken on the spare panel. The results are presented as maps of the absorptance distribution and homogenous zones.

Table 1 summarizes the results of the measurements made of the whole receiver, the fifth panel, and the new panel.

The second measurement campaign (January 1986) showed a mean absortance of 95.3% for the whole panel and 95.7% for the fifth panel.

The variance analysis for a confidence level of 95%, gives the three zones plotted in Figure 1. This figure also presents the values within, below, and above the mean for the whole receiver.

Figure 2 shows the three-zone representation for the fifth panel in January 1985; Figure 3 shows the same representation for January 1986. A small variation is noted in the absorptance measurement on the fifth panel after having operated at solar fluxes as high as 2.5 MW/m^2.

The optical losses can be determined either from the incident power to the receiver:

$$L_o = Q_{in}(1-\alpha) \qquad (1)$$

or from the collected power by the sodium and the thermal losses:

$$Q_{abs} = Q_{coll} + L_t \quad (2)$$

$$Q_{abs} = \alpha \cdot Q_{in} \quad (3)$$

Solving (1), (2), and (3),

$$L_o = (Q_{coll} + L_t)\ (1/\alpha - 1) \quad (4)$$

where Q_{in} = incident solar power reaching the receiver
Q_{abs} = power absorbed by the panel
Q_{coll} = power gained by the sodium
L_t = thermal losses of the receiver

3. THERMAL LOSSES

3.1 Description of the Experiments

A review of the possible techniques to measure thermal losses is presented in (Ref.1). Because of the greater accuracy, the preferred method is the flux-off procedure. The tests consist simply in circulating sodium through the receiver with the doors open at different inlet temperatures and wind speeds. To cover the whole range of operating temperatures, two procedures have been selected.

Normal flow operation. This procedure has been used to test the receiver with inlet temperatures from 200°C to 300°C. The flowrate remains constant by manipulating the sodium pump speed. The sodium flows from the cold tank to the hot tank through the receiver until reaching steady-state. The total losses are calculated measuring the enthalpy loss of the sodium.

Reverse flow operation. Due to operating constraints, the receiver cannot be operated with an inlet temperature higher than 300°C in normal flow. The experiment consists in circulating hot sodium from the hot tank to the cold tank in the reverse flow direction. Since the pump cannot operate in reverse flow, the flowrate must be manually controlled by regulating the difference of argon pressure between the tanks.

The inlet and outlet thermocouples were carefully calibrated (Ref.2) and a differential thermocouple circuit was installed between the receiver inlet and outlet to increase the accuracy of the measurements of this temperature

difference. The flowmeter installed for measuring the sodium flowrate is a magnetic type. A root-sum-square uncertainty analysis shows an error of 3% in the calculations of the energy lost during the tests.

3.2 Total Losses

As previously noted, thermal losses are calculated from the variation of the sodium enthalpy through the receiver.

$$L_t = v \cdot \rho \cdot \int_{T_i}^{T_o} C_p \, dT \qquad (5)$$

where v = sodium flowrate (m^3/s)
T_i = inlet temperature (°C)
T_o = outlet temperature (°C)
ρ = sodium density (kg/m^3)
C_p = specific heat (kJ/kg°C)

The sodium density and specific heat are temperature dependent.

$$\rho = C_1+T_i(C_2+T_i(C_3+T_iC_4))$$

where C_1 = 950.07
C_2 = -0.229
C_3 = $-1.46\ 10^{-5}$
C_4 = $5.638\ 10^{-9}$

$$C_p = a_1(a_2+T(a_3+a_4T))$$

where T = sodium temperature (°C)
a_1 = $4.187\ 10^{-3}$
a_2 = 343.24
a_3 = -0.1387
a_4 = $1.1044\ 10^{-4}$

To determine the losses in the receiver, a set of 30 tests have been performed; 15 in the reverse flow mode. During the tests, the mean sodium temperature over ambient temperature (ΔT) ranged from 172°C to 377°C. Under normal operating conditions, this mean temperature is about 380°C (T_i = 270°C, T_o = 530°C, T_∞ = 20°C).

From the existing data and the application of (5), the total losses were calculated. Using a polynominal fitting, the following expression has been determined:

$$L_t = 34.6 - 0.18\,\Delta T + 0.0015\,\Delta T^2 \qquad (6)$$

where $r^2 = 0.934$

This fit is not as good as could be expected, because the wind effect is not considered. The wind effect on the convective coefficient will be presented later. Figure 4 shows the losses for the data points and the polynominal expression.

The mean sodium temperature has been assumed to be representative of the mean receiver surface temperature. This is justified when there is no concentrated power incident on the receiver. It is estimated that the difference between the bulk medium temperature in the receiver pipe and the outside pipe temperature is about 2°C. These estimates agree with the data obtained from the infrared thermography measurements carried out by DFVLR during the measurement campaign in October 1985 (Ref.3). Table 2 shows the comparison of the sodium temperature and the surface temperature measured by the infrared camera during a reverse flow test on October 31, 1985.

3.3 Radiative Losses

Calculation of radiative losses from billboard receivers is relatively straightforward. The receiver loses thermal energy by radiating to its surroundings.

$$L_r = \varepsilon\, A\sigma(0.5(T_m^4 - T_s^4)) + (0.5(T_m^4 - T_\infty^4)) \qquad (7)$$

The IR radiation, L_r, is split between the sky and the ground. The ground is assumed to be at ambient temperature, T_∞. A relationship between sky and ambient temperature is described by Berdahl and Fromberg (Ref.4).

$$T_s = \varepsilon_s^{0.25} T \qquad (8)$$

where ε_s is the sky emissivity which has been correlated with the dewpoint temperature (Ref.4).

$$\varepsilon_s = 0.741 + 0.0062\, T_{dwpt} \qquad (9)$$

The surface properties of the Pyromark coating are responsible for the amount of absorption and emission. A scalloped surface like a tube panel produces an effective emissivity larger than that of a flat surface. The correlation for a tube panel with no space between the tubes can be written as:

$$\varepsilon_{eff} = \varepsilon / (1-(1-\varepsilon)(1-2/\pi)) \qquad (10)$$

The losses by emission are based on calculations made using an effective emissivity in the infrared wavelength of $\varepsilon_{eff} = 0.90$ (Ref.5).

From the data of the set of experiments described in the last section, and applying (7), the radiative losses have been calculated and plotted in Figure 5. These losses fit the following expression:

$$L_r = 35 - 0.28\,\Delta T + 0.00106\,\Delta T^2 \qquad (11)$$

where $r^2 = 0.996$ in the range $150°C < \Delta T < 400°C$.

A comparison has been made between the radiative losses based on calculation through the application of (11), and those based on the infrared thermography measurements; the results are shown in Table 2. It can be stated that the agreement is good. Equation (7) is used to determine radiative losses during normal operation, since correlation (11) is valid only when the incident radiation on the receiver is 0.

3.4 Conductive Losses

Conductive losses for central receivers are often neglected or considered a small fraction of the total losses. The conduction can be determined within a large margin of error by calculating the losses as a function of the thermal conductivity and the difference of temperatures through the insulation or by operating the receiver with the doors closed. In both cases, conductive losses of less than 5% have been determined. For the rest of this paper, a conductive loss of 5% of the total thermal losses will be assumed.

$$L_{cd} = 0.05\ L_t \qquad (12)$$

3.5 Convective Losses

Convection loss tests were run by simply opening the doors of the receiver without providing any incident power from the heliostat field. After reach-

steady-state conditions, the convective losses may then be determined by:

$$L_c = L_t - L_r - L_{cd} = 0.95\ L_t - L_r \qquad (13)$$

The total thermal losses and the radiative losses have already been calculated. Therefore, the convective losses can be determined from (13).

Figure 6 shows the convective losses for different mean temperatures. Due to the different operating conditions during the tests, a great dispersion is observed.

3.6 Convective Coefficient

One of the goals of this experiment is to determine the convective coefficient for different wind speeds. To do this, a second set of experiments were carried out with the ASR. The operating conditions were carefully selected. The tests were run with wind blowing only parallel to the receiver surface: an East-West direction, also the predominant wind direction on site. The inlet temperature was maintained between 270°C and 285°C for all the tests, and the wind speeds of up to 75 km/h were obtained.

A set of 18 tests were carried out in the abovementioned conditions. The convective losses were calculated according to (13) and the convective coefficient, h was calculated:

$$h = \frac{L_c}{A \cdot \Delta T} \qquad (14)$$

where A is the receiver surface (2.75 x 2.85 m).

The values of h measured versus wind speed, V, are plotted in Figure 7. A good fit is noted with the polynominal expression

$$h = 14.0 + 0.928\ V + 0.056\ V^2 \qquad (15)$$

with a determination coefficient of 0.989.

The convective heat transfer process in the receiver is characterized by mixed convection, a combination of both natural and forced convection. It is of interest to predict this coefficient and compare it to the measured one.

A correlation proposed by Siebers and Kraabel (Ref.6) is used to determine the mixed convective coefficient.

$$h = (h^a_{nat} + h^a_{forc})^{1/a} \tag{16}$$

where a = 1 for laminar regime, and 3.2 for turbulent regime.

To calculate the natural convective coefficient, a correlation proposed by McAdams (Ref.7) has been used.

$$h_{nat} = 1.42\ (\Delta T/l)^{1/4} \tag{17}$$

for laminar regime (10^4 Rayleigh number 10^9)

$$h_{nat} = 1.31\ \Delta T^{1/3} \tag{18}$$

for turbulent regime (10^9 Rayleigh number 10^{13})

The forced convective coefficient has been calculated using the following correlation (Ref.8)

$$Nu = 0.6795\ Re^{1/2} Pr^{1/3} (T_m/T_\infty)^{0.4} \quad \text{for } Re < 5 \cdot 10^5 \tag{19}$$

$$Nu = 0.037\ Re^{0.8} Pr^{0.6} (T_m/T_\infty) \quad \text{for } Re \geq 5 \cdot 10^3 \tag{20}$$

From the Nusselt number, the forced convective coefficient

$$h_{forc} = Nu \cdot K_{air}/l \tag{21}$$

where K_{air} = air conductivity calculated at film temperature
l = 2.75 m (characteristic length)

The predicted convective coefficient is plotted against the measured convective coefficient in Figure 8. The dashed line indicates perfect agreement between the predicted and measured coefficient. As shown, the agreement is quite good considering the uncertainties in the correlations used and errors in the instrumentation.

4. CALCULATION PROCEDURE USED TO DETERMINE LOSSES DURING OPERATION

Based on the determination of the losses described in the previous sections, total losses and receiver efficiency during normal operation can be calculated. The procedure used is as follows:

(A) Take the following data from the Data Acquisition System:

- inlet and outlet receiver sodium temperatures
- sodium flowrate
- ambient temperature
- wind speed

(B) Determine the mean temperature of the receiver surface as:

$$T_m = (T_i+T_o)/2$$
$$\Delta T = T_m - T_\infty$$

(C) Calculate the radiative loss using Equation (7).

(D) Calculate the convective coefficient using Equation (15).

(E) Calculate the convective loss applying Equation (14).

(F) Calculate the thermal losses using Equation (13), e.g.,

$$L_t = (L_r+L_c)/0.95$$

(G) The power gained by the sodium is calculated from Equation (5), where the temperature difference is achieved by changing '(T_i-T_o)' in the first case to '(T_o-T_i)' in the second.

(H) The optical losses are calculated using Equation (4).

As an example, in the following thermal losses and receiver efficiency are calculated for the receiver operating under steady-state conditions on November 8, 1985 at 11:45 (solar time).

(A) Irradiance : 962 W/m^2
Flowrate : 40.9 m^3/h
Inlet temperature : 280°C
Outlet temperature : 555°C
Ambient temperature : 29°C
Wind speed : 12.6 km/h

(B) Mean temperature of the receiver over ambient is 417.5°C.

(C) The radiative loss is 89 kW.

(D) The convective coefficient is 17.9 W/m^2°C.

(E) The convective loss is 54.6 kW.

(F) The thermal losses are 151 kW.

(G) The power gained by the sodium is 3534 kW.

(H) The optical loss is 193 kW.

The receiver efficiency may then be calculated as:

$$\eta = \frac{Q_{coll}}{Q_{coll}+L_t+L_o} = 0.911$$

The radiant losses of the receiver were measured using the Infrared Imaging System installed on site. To verify the model during normal receiver operation, representative temperature measurements were taken of the receiver and radiation losses determined, using the infrared camera. The results of this evaluation follow.

5. RESULTS AND CONCLUSIONS

Table 3 presents the predicted thermal losses of the tests performed on 29 July, and 4, 6, 7, and 8 August, 1986. This table includes the mean receiver temperature; the radiation, convective, total, and optical losses; total absorbed power; and receiver efficiency.

Table 4 presents results obtained through evaluation of the images taken with the infrared system on the days previously cited, along with the prediction of these parameters. The agreement between actual and predicted results is very good.

Table 5 compares the results obtained using this model and those of other investigators (Ref.9). The results are very similar with the exception of the receiver efficiency, where a more realistic value is obtained with the present model.

The efficiency value determined using this model was compared with that obtained by the verified simulation program of the receiver (Ref.10); the results proved to be consistent (Table 6).

Finally, it should be noted that the method used to determine global thermal losses of the ASR is easy to use and offers results very similar to those found in other tests and simulation programs.

6. REFERENCES

1. Kraabel, J.J., 'Convection Testing of the Central Receiver System', IEA-SSPS Technical Report 4/83, DFVLR, Cologne (1983).

2. Brinner, A., 'Recalibration of Relevant Temperature Sensors and Sodium Flowmeters at SSPS/CRS', IEA-SSPS Technical Report 4/84, DFVLR, Stuttgart (1984).

3. Schiel, W., DFVLR Stuttgart, personal communications.

4. Berdahl, P. and Fromberg, R., 'The Thermal Radiance of Clear Skies', Solar Energy, vol. 29, pp. 299 (1982).

5. Lemperle, G., 'Results of a Numerical Simulation and Surface Temperature Measurements', Internal Report, IB-444-006/85, DFVLR, Stuttgart (1985).

6. Siebers, D. and Kraabel, J.J., 'Estimating Convective Energy Losses from Solar Central Receivers', Proceedings of the IEA Workshop, San Diego, Cal., June 10-14, 1984.

7. McAdams, W.H., 'Transmisión de Calor', McGraw-Hill, New York (1954).

8. Siebers, D., 'Natural Convection Heat Transfer from Ext. Rec.', SAND78-8276.

9. Baker, A.F., 'Loss Tests by Complementary Heliostat Field Configurations', IEA-SSPS Internal Report R-39/86AB.

10. Rosa, F., 'Thermodynamic Simulation of the ASR using 'THERESA'', IEA-SSPS Internal Report R-36/86FR.

	number of samples	mean value (%)	standard deviation
whole receiver	165	95.8	0.33
fifth panel	189	95.7	0.35
new panel	62	96.6	0.26

Table 1

time	mean sodium temperature (°C)	mean surface temperature (°C)	Radiative losses (kW) from: sodium data	IR camera
14:13:18	372	368	66	65.5
14:20:30	373	330	67	66
14:42:42	397	395	77	77

Table 2

TEST	MEAN TEMP.(C)	RAD. LOSSES(KW)	CONV. LOSSES(KW)	THERMAL LOSSES(KW)	OPT. LOSSES(KW)	ABS. POWER(KW)	EFFICIENCY
72901	399.0	79.75	64.03	151.35	117.08	2073.13	.885
72902	399.2	79.85	72.40	160.27	117.81	2078.20	.882
72903	401.7	81.07	70.40	159.18	119.75	2116.02	.883
72904	399.45	79.97	75.43	163.58	117.12	2061.61	.880
72905	399.45	79.97	68.17	155.94	115.69	2042.12	.882
80402	396.05	78.33	75.20	158.78	125.9	2233.37	.886
80403	396.35	78.47	56.75	142.35	124.58	2224.75	.893
80404	396.35	78.47	59.15	144.86	120.50	2144.54	.890
80405	398.10	79.32	54.73	141.10	102.45	1805.40	.881
80406	397.35	78.95	64.40	150.90	104.71	1838.59	.878
80601	402.25	81.34	60.11	148.90	118.98	2111.64	.887
80602	401.60	81.02	57.54	145.86	117.29	2082.56	.887
80603	402.05	81.24	53.63	141.98	115.21	2047.02	.888
80604	402.05	81.24	62.59	151.41	113.41	2003.35	.883
80605	402.95	81.69	69.59	159.16	115.23	2030.20	.880
80606	402.05	81.24	67.93	157.03	115.63	2039.87	.882
80702	401.15	80.80	66.42	154.97	112.63	1985.02	.881
80703	402.75	81.59	66.71	156.11	115.58	2039.95	.882
80704	401.35	80.90	66.46	155.11	114.30	2016.68	.882
80801	399.20	79.85	51.09	137.83	140.06	2523.30	.900
80802	401.75	81.10	50.38	138.40	143.44	2587.00	.902
80803	401.05	80.75	61.14	149.36	144.06	2588.00	.898
80804	401.55	81.00	56.38	144.62	144.04	2592.07	.900
80805	401.25	80.85	46.65	134.21	141.72	2558.41	.902
80806	400.85	80.66	52.65	140.32	141.62	2550.53	.900
80807	401.10	80.78	62.43	150.75	140.58	2520.23	.896
80808	401.10	80.78	51.35	139.09	139.29	2507.42	.900
80809	403.10	81.76	53.22	142.09	138.71	2493.33	.898

TABLE 3: M O D E L R E S U L T S

	FROM THE MODEL		FROM THE INFRARED SYSTEM	
TEST	MEAN TEMP.(C)	RAD. LOSSES(KW)	MEAN TEMP.(C)	RAD. LOSSES(KW)
72901	399.0	79.75	397.30	88.4
72902	399.2	79.85	397.80	88.8
72903	401.7	81.07	402.10	90.6
72904	399.45	79.97	403.30	91.2
72905	399.45	79.97	400.40	89.6
80402	396.05	78.33	387.80	83.5
80403	396.35	78.47	391.80	87.0
80404	396.35	78.47	392.70	86.4
80405	398.10	79.32	382.20	80.6
80406	397.35	78.95	397.20	86.6
80601	402.25	81.34	380.60	79.6
80602	401.60	81.02	381.50	80.5
80603	402.05	81.24	378.70	78.2
80604	402.05	81.24	377.40	77.9
80605	402.95	81.69	380.40	79.6
80606	402.05	81.24	376.50	77.8
80702	401.15	80.80	391.60	85.9
80703	402.75	81.59	390.30	83.2
80704	401.35	80.90	388.10	82.9
80801	399.20	79.85	367.90	74.3
80802	401.75	81.10	376.90	79.1
80803	401.05	80.75	378.70	79.8
80804	401.55	81.00	370.20	75.5
80805	401.25	80.85	378.90	79.6
80806	400.85	80.66	379.30	80.3
80807	401.10	80.78	381.90	81.3
80808	401.10	80.78	397.60	88.4
80809	403.10	81.76	394.50	86.5

TABLE 4:COMPARISON OF MODEL WITH THE INFRARED SYSTEM

DATE	MEAN TEMP.(C) PRED/BAKER'S MOD.	RAD. LOSSES(KW) PRED/BAKER'S MOD.	CONV. LOSSES(KW) PRED/BAKER'S MOD	THERMAL LOSSES PRED/BAKER'S MOD	EFFICIENCY PRED/BAKER'S MOD.
9/24/85	399.5/372.	80.2/76.5	45.0/36.3	132.0/112.8	.897/.923
9/27/85	403.5/387.	82.1/83.0	45.0/37.0	133.8/120.0	.905/.928
10/3/85	403.5/395.	82.0/86.6	52.5/43.4	129.5/129.9	.895/.919
10/16/85	342.5/342.	55.8/64.5	40.3/33.6	101.2/98.1	.920/.940
10/17/85	346.5/340.	57.3/63.5	60.9/57.2	124.5/120.7	.907/.927

TABLE 5: COMPARISON OF MODEL WITH BAKER'S MODEL

TEST	EFFICIENCY	
	MODEL	'THERESA'
72901	.885	.899
72902	.882	.889
72903	.883	.892
72904	.880	.885
72905	.882	.893
80402	.886	.899
80403	.893	.911
80404	.890	.911
80405	.881	.891
80702	.881	.908
80703	.882	.916
80704	.882	.916
80801	.900	.907
80802	.902	.910
80803	.898	.901

TABLE 6: COMPARISON OF MODEL WITH 'THERESA' RESULTS

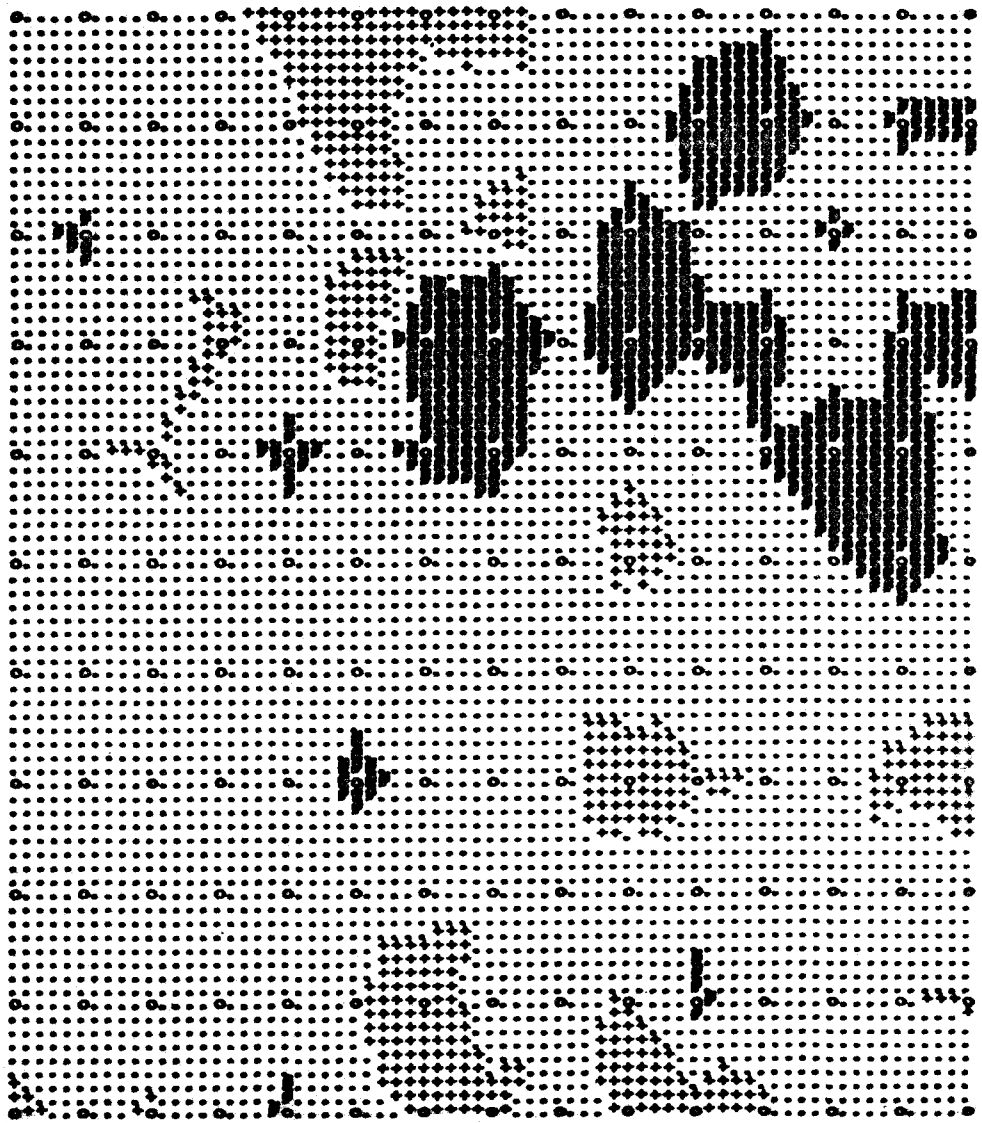

RECEIVER PLOTTER ASR

ABSORTIVITY DISTRIBUTION
SSPS. ALMERIA

MLRAD COMPUTER PROGRAM

DATE : JANUARY/ 85

MEDIUM ABS: 95.8 %

SCALE

SIMBOL	ABSX
+	UP MEDIUM
-	AROUND MEDIUM
#	DOWN MEDIUM
o	MEASUREMENT POINTS

Figure 1

ABSORTIVITY DISTRIBUTION ON THE 5th PANEL. ASR

DATE : JAN 1985- AVERAGE ABSORTIVITY: 95.79%

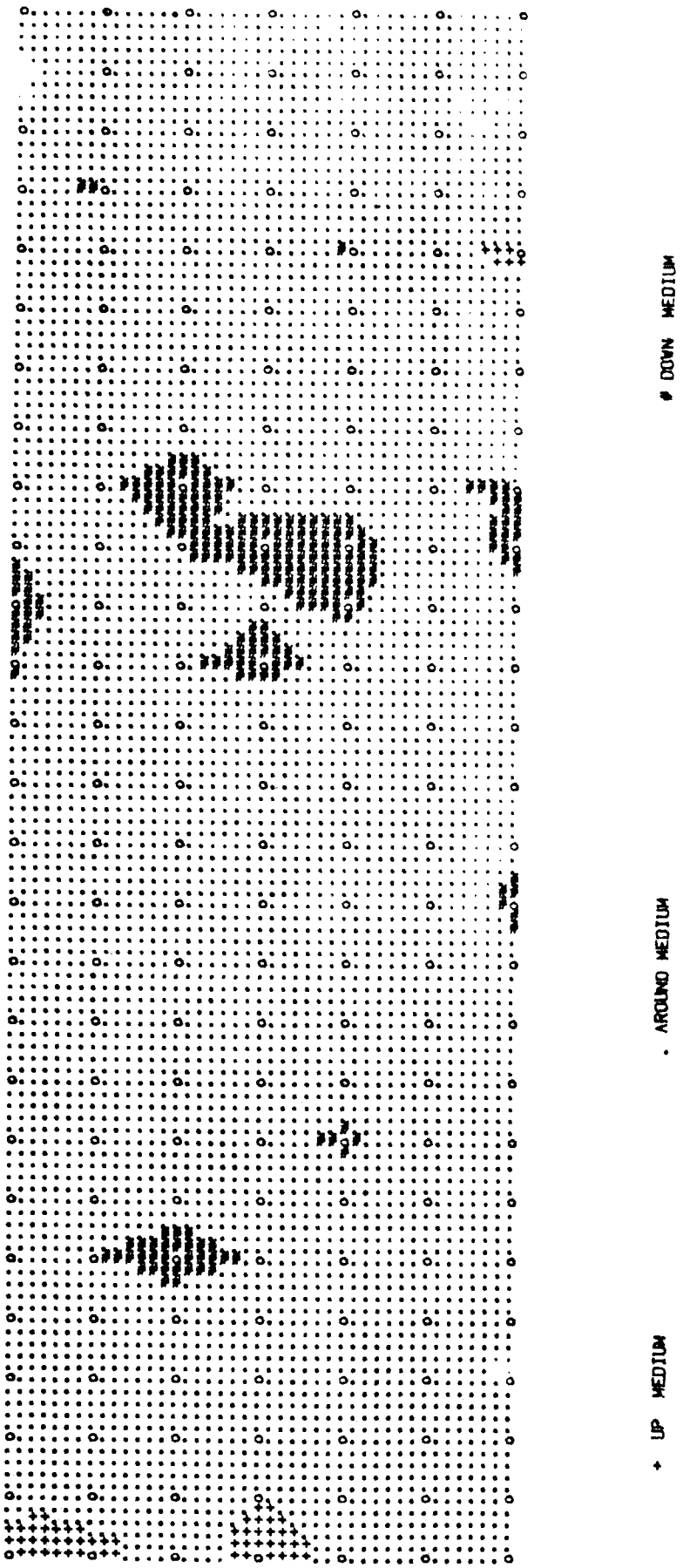

Figure 2

ABSORTIVITY DISTRIBUTION ON THE 5th PANEL. ASR

DATE : JAN, 1986 AVERAGE ABSORTIVITY: 95.789%

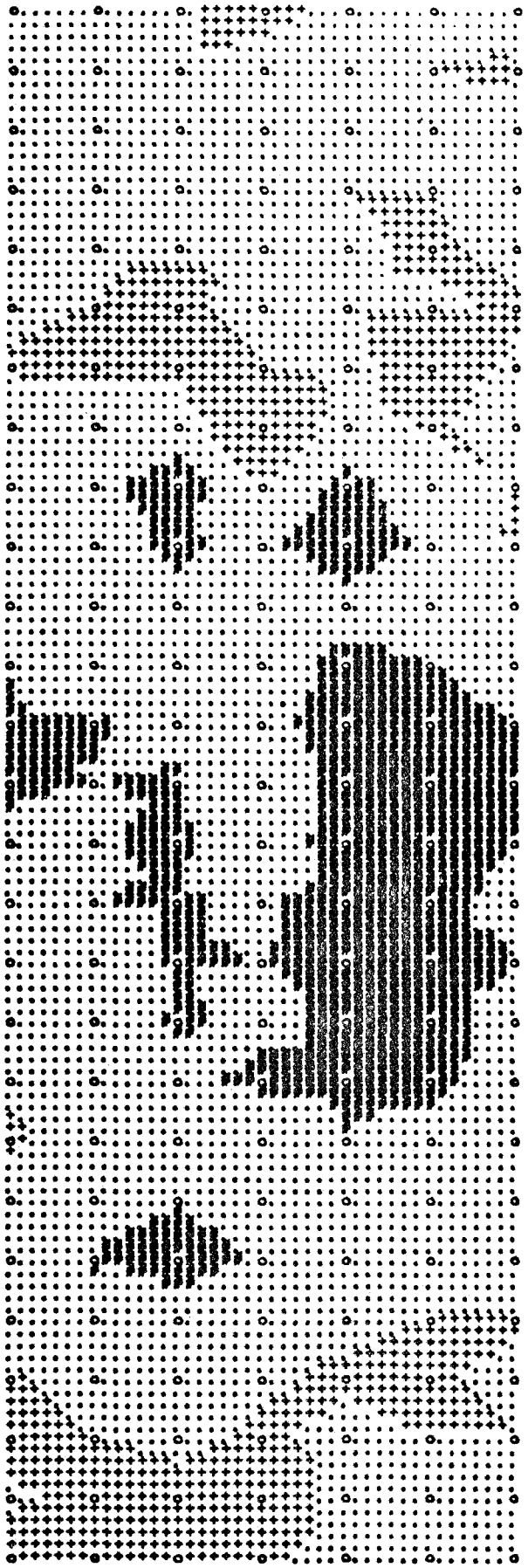

Figure 3

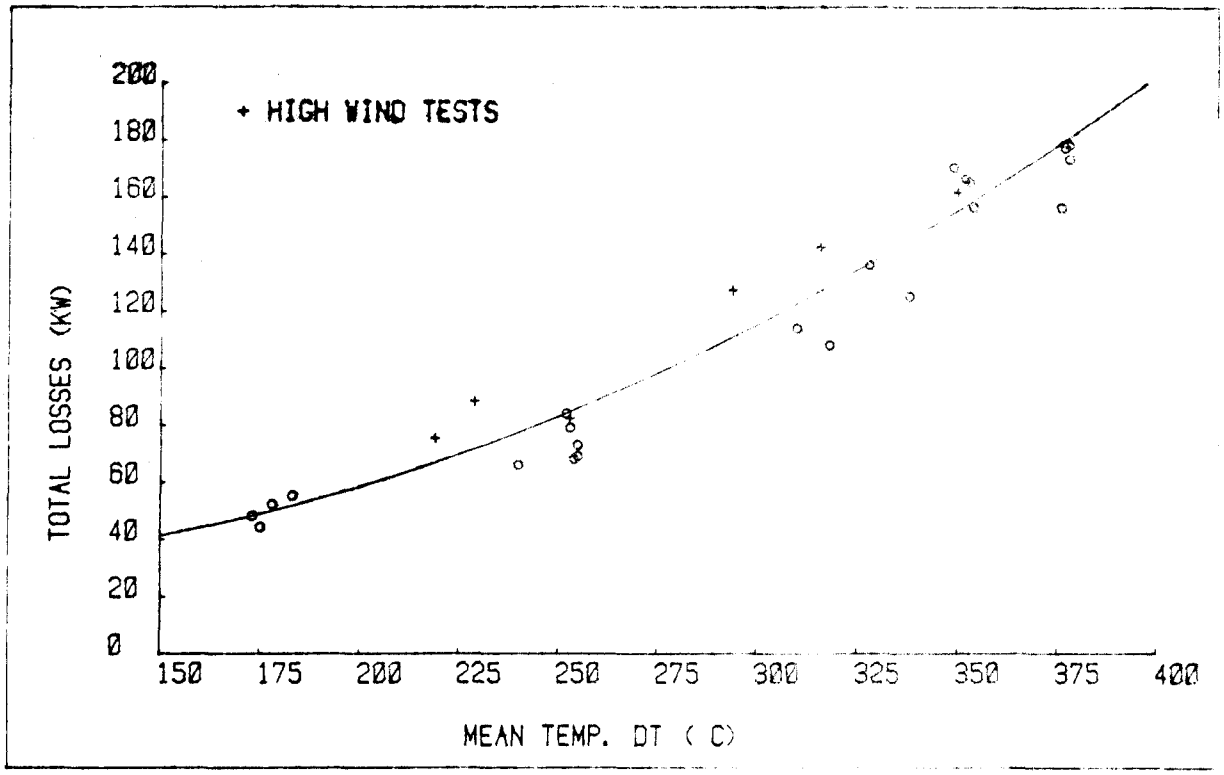

Figure 4

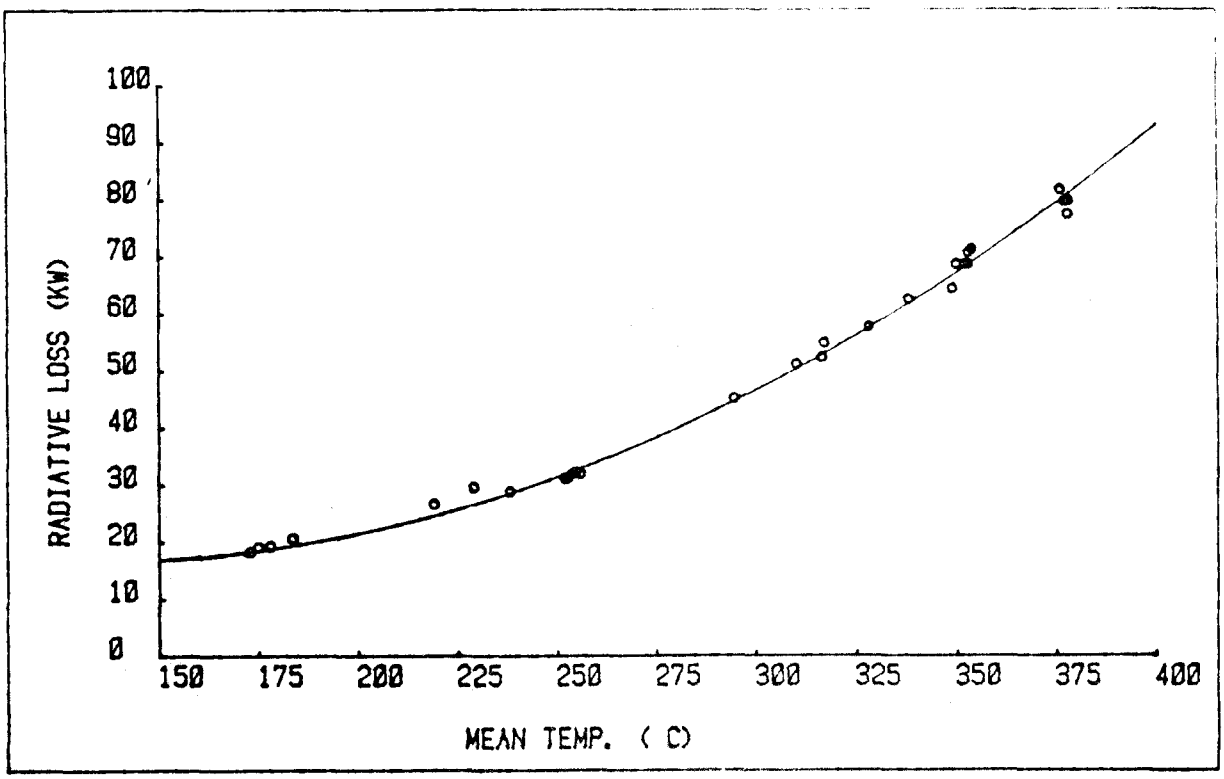

Figure 5

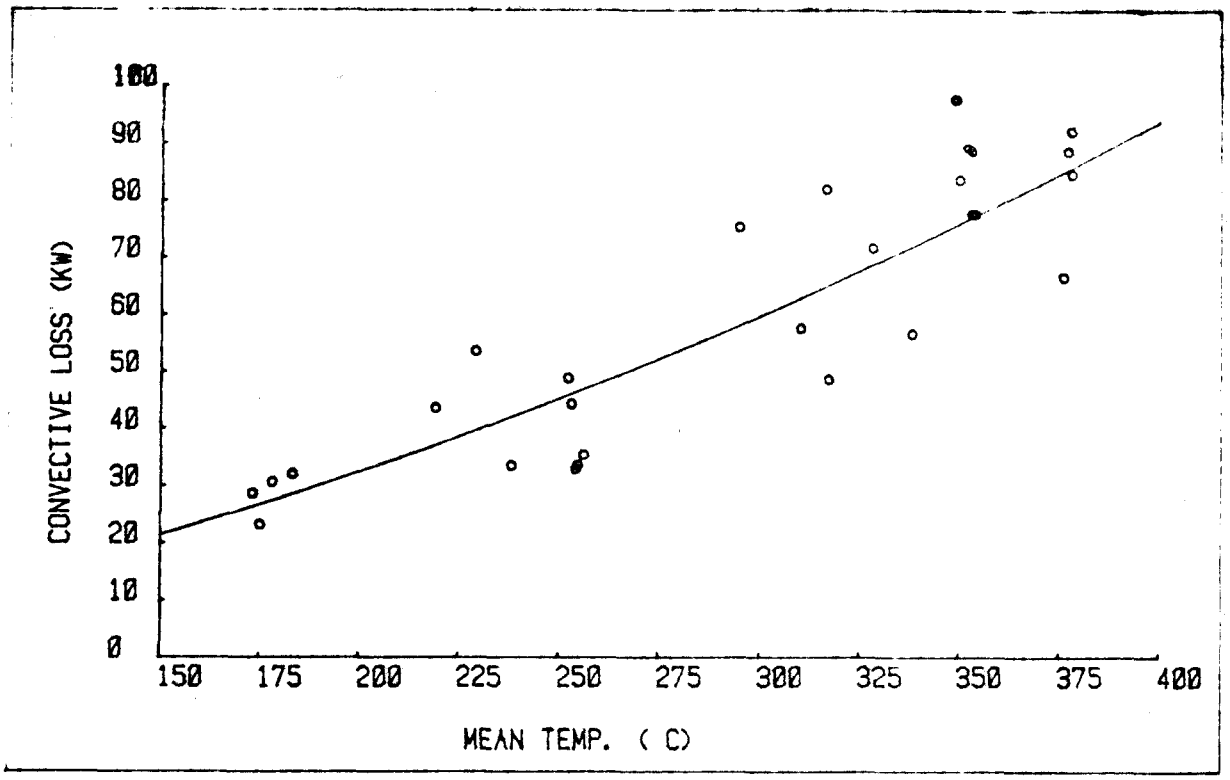

Figure 6

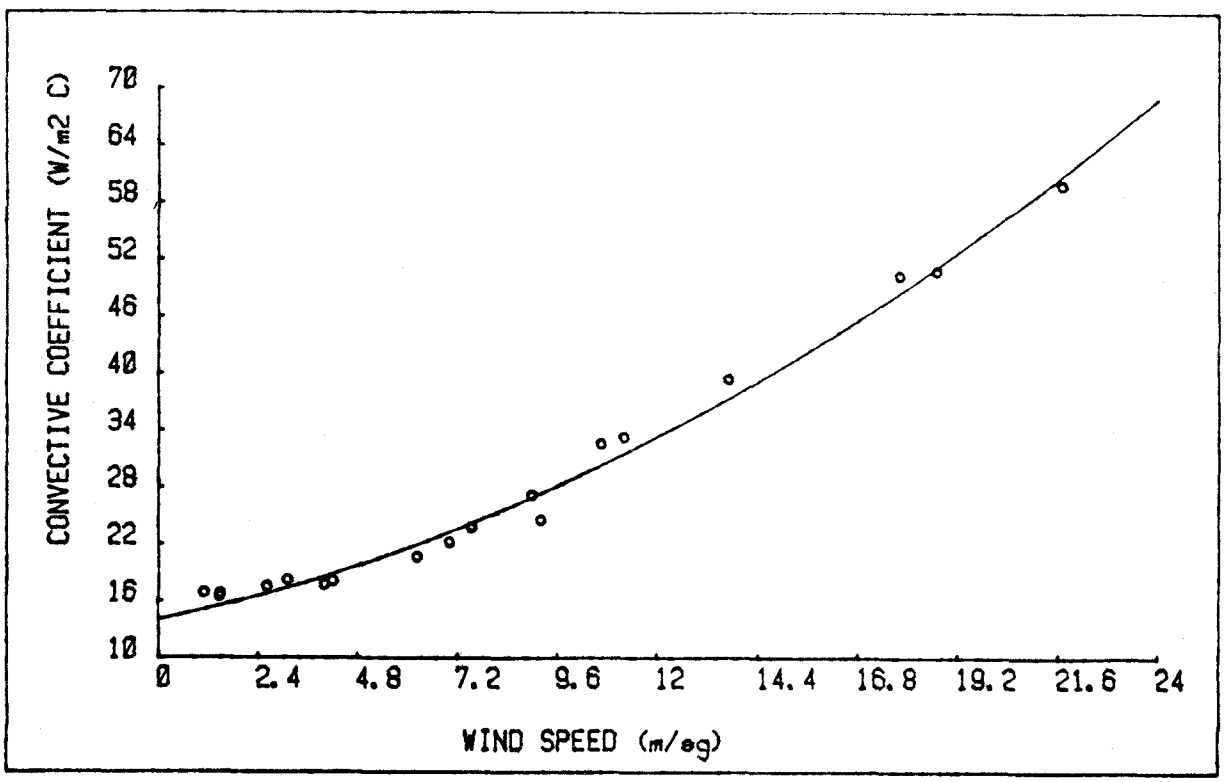

Figure 7

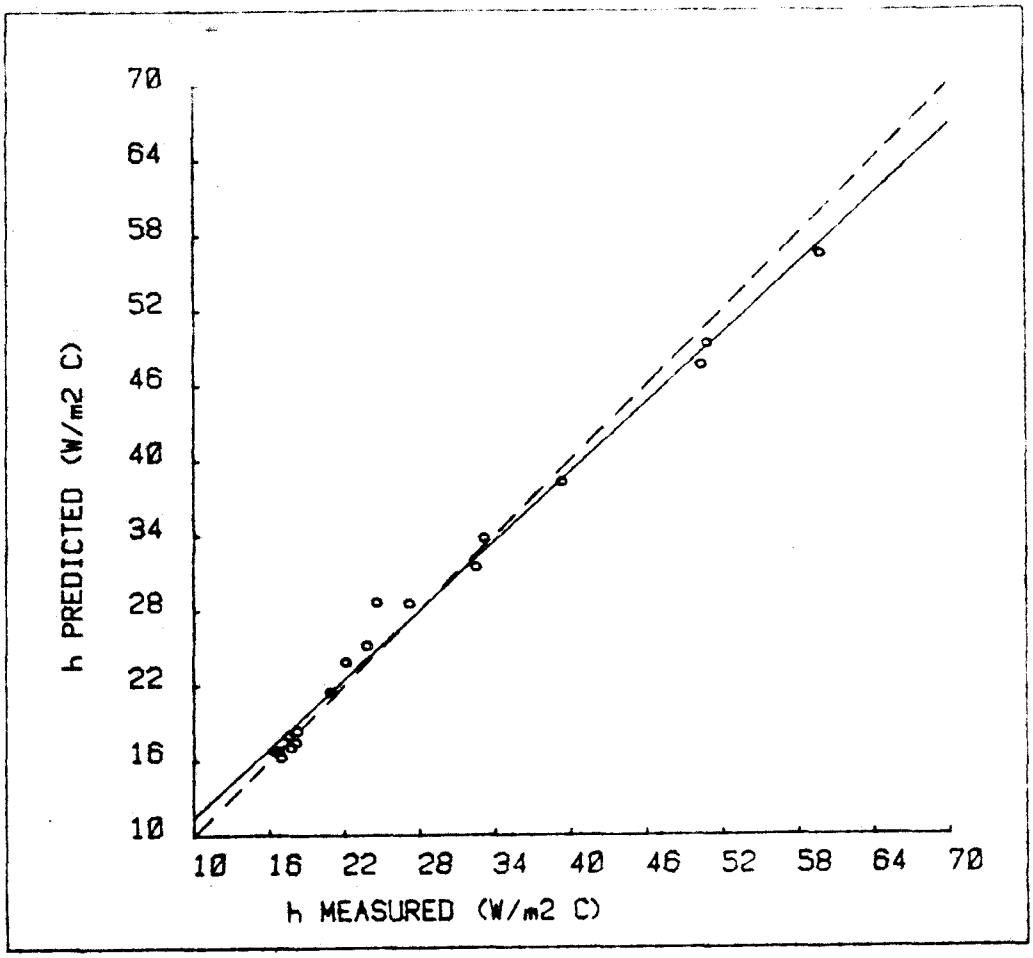
70
64
58
52
46
40
34
28
22
16
10
h PREDICTED (W/m2 C)
10
16
22
28
34
40
46
52
58
64
70
h MEASURED (W/m2 C)

Figure 8

DISTRIBUTION

1. Members of the Executive Committee
   - C.-J. Winter (D)
   - G. Faninger (A)
   - F. Altdorfer (B)
   - P. Kesselring (CH)
   - W. Rasch (D)
   - L. Crespo Rodriguez (E)
   - F. Reale (I)
   - B. Finnström (S)
   - Ch. Carwile (USA)

2. IEA Secretariat
   - P.J. Heinzelmann

3. BMFT / KFA-PLE
   - H. Eisenbeiss
   - F. Friedrich

4. DFVLR
   - W. Grasse - E.C. Secretary (5X)

5. Junta de Andalucia - Director General de Industria y Energía
   - M. Martín

6. Junta de Andalucia - Consejería de Industria y Energía, Almería
   - J. Mesas

7. Junta de Energía Nuclear - Instituto de Energias Renovables
   - J.A. Azuara Solís
   - J. Avellaner Lacal (IDAE)
   - A. Rodrigo Otero
   - J.M. Rubio
   - F.S. Sánchez Sudón - Operating Agent

8. ASINEL
   - J.M. Fluxá Ceva
   - J. de Marcos Peñalba

9. US-DOE / SANDIA / SERI
   - F. Morse
   - A. Baker
   - A. Skinrood
   - L. Gutierrez
   - B. Gupta

10. Cía. Sevillana de Electricidad
    - J.M. González Moreno

11. Contractors
    - ACUREX
    - AGIP
    - ELECTROWATT
    - FRANCO-TOSI
    - INTERATOM
    - MAN-NT
    - MARTIN MARIETTA
    - MOMPRESA
    - SAIT
    - SULZER
    - TECNICAS REUNIDAS

12. Director, Plataforma Solar (Almería) (8X)
    - C. Arañó

13. Universidad de Sevilla
    - V. Ruiz